



Novel monolithic “Slightly-Open doormat” (SOD) valve enables efficient fabrication of highly-scalable microfluidic gas-on-gas multiplexer



Priyan Weerappuli^{a,b,c,*}, Taisuke Kojima^{b,c,d}, Shuichi Takayama^{b,c,d}, Amar Basu^{a,e}

^a Department of Biomedical Engineering, Wayne State University, Detroit, MI 48202, USA

^b Department of Biomedical Engineering, University of Michigan, Ann Arbor, MI 48109, USA

^c Biointerfaces Institute, University of Michigan, Ann Arbor, MI 48109, USA

^d Department of Biomedical Engineering, Georgia Institute of Technology, Atlanta, GA 30332, USA

^e Department of Electrical and Computer Engineering, Wayne State University, Detroit, MI 48202, USA

ARTICLE INFO

Keywords:

Microfluidics
Elastomeric valve
Monolithic PDMS valve
Large-Scale integration
Multiplexer
Microvalve
Normally-Closed valve
Normally-Open valve

ABSTRACT

The use of monolithic normally-closed (NC) valves within microfluidic systems is currently limited by the poor scalability of mitigation strategies developed to prevent the formation of a permanent bond between the valve ‘seat’ and elastomeric membrane during fabrication. Herein we report the highly-scalable design and characterization of a slightly-open doormat (SOD) valve that exhibits properties traditionally associated with NC valves including operability at low actuation pressures, and the capacity to produce a complete seal. In addition, these valves are comparable in their scalability and in responsiveness, and exhibit a capacity to eliminate resting channel resistance that is absent in their NC counterparts. We demonstrate the utility of this novel valve design through the design and operation of a gas-on-gas multiplexer containing 32 device valves controlled by a multiplexer containing 160 SOD valves using only 10 external solenoid valves and a single common pressure source.

1. Introduction

In academic parlance, the term microfluidics refers to a discipline concerned with the study and development of engineered systems capable of effectively handling sub-milliliter volumes of fluid. The progeny of technologies pioneered with pulled glass capillary tubes (e.g. the Coulter counter); most modern microfluidic systems are fabricated using the silicone polymer polydimethylsiloxane (PDMS) and, despite tending toward planar geometries, boast greater degrees of operational complexity than their antecedents owing to the ability of this material to support elaborate channel architectures and integrated control elements [1]. Of the numerous control elements developed to date, perhaps none has proven as transformational as the elastomeric microvalve – a monolithic control element that enables the movement of fluid through a channel to be interrupted, diverted, or metered by the distension of a flexible membrane.

The taxonomy of microvalve designs can be classified into two distinct sub-groups, based upon their resting state: *normally-open* (NO) and *normally-closed* (NC) (Fig. 1). NO microvalves, of which the Quake bilayer microvalve represents the most common embodiment, consist of paired hemi-circular channels cast in separate layers of PDMS [2]. By

stacking these layers such that the channels are oriented orthogonal to one another, an increase in pneumatic pressure within one channel (the *control* channel) may be made to produce distension of the diaphragm-like region separating it from the other channel (the *flow* channel) [2,3].

NC microvalves (Fig. 1), of which the Hosokawa and Maeda ‘doormat’ valve represents the most common embodiment [4], differ from NO microvalves in that while they are also comprised of orthogonally oriented paired channels, these channels are assembled in vertical juxtaposition to one another (both channelled sides facing inward), and are bonded to opposite sides of a third elastomeric diaphragm layer. These valves differ, also, in that flow channels are discontinuous at points where valves occur. The presence of these discontinuities forces the movement of fluid within a channel to either stagnate upstream of these points, or to continue downstream by distension of the elastomeric diaphragm layer. Though a subtle modification in design, the presence of this discontinuity effectively allows NC valves to be operated at lower pressures and higher frequencies than their NO counterparts, and to better isolate upstream and downstream fluid compartments.

Despite their advantages, NC valves have seen relatively infrequent

* Corresponding author at: Department of Biomedical Engineering, Wayne State University, Detroit, MI 48202, USA.

E-mail address: pweerapp@umich.edu (P. Weerappuli).

<https://doi.org/10.1016/j.snb.2019.126776>

Received 9 December 2018; Received in revised form 2 July 2019; Accepted 3 July 2019

Available online 03 July 2019

0925-4005/ Published by Elsevier B.V.

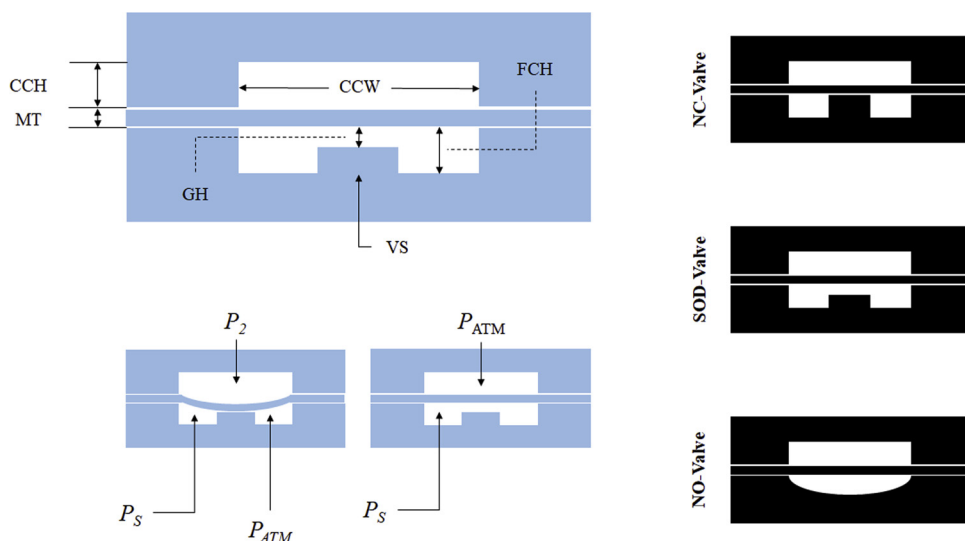


Fig. 1. A schematic of the SOD valve (left) with the control channel height (CCH), elastomeric membrane thickness (MT), actuation/control chamber width (CCW), gap-height (GH), valve seat (VS), and flow channel height (FCH) indicated. Closure of the valve is achieved by modulating the pressure within the actuation chamber (P_2) such that $P_2 > P_{ATM}$ and the downward force exerted on the elastomeric membrane by P_2 exceeds the upward force applied to the membrane by the upstream source pressure (P_S). Cross-sectional diagrams of the SOD valve in relation to conventional NC- and NO-valves (right) is included to illustrate the fundamental difference between these designs.

use, due to challenges with membrane stiction during fabrication. The bonding of PDMS layers is commonly achieved through the treatment of bonding surfaces using oxygen plasma [5,6]. Exposure to oxygen plasma results in a depletion of surface CH_3 and CH_2 functional groups, and a concomitant enrichment of surface silanol ($\text{Si}-\text{OH}$) groups [7]. When two bonding surfaces are brought into contact with one another, silanol groups on opposing surfaces undergo condensation reactions – forming a permanent bond between these surfaces. The challenge this presents for the fabrication of NC valves stems from the contact that must be made between the plasma-exposed channel discontinuity (the valve ‘seat’) and the plasma-exposed elastomeric membrane without these structures forming a permanent bond.

Historically, several approaches have been taken to address this challenge including the use of microcontact stamps to deposit residual PDMS oligomers on valve seat regions following plasma treatment [8]; the use of a ‘shadow mask’ [9] or solid ‘shelter’ [10] to exclude surface regions from being exposed to plasma during treatment; the deposition of metallic/polymeric sacrificial materials in regions from where they may be removed following bonding of the two layers [11]; the use of partially-cured PDMS membranes that will be prone to stick to the valve ceiling during final device assembly [12]; and the application of negative pressure during bonding to prevent contact between these regions until complete hydrophobic recovery has occurred [13,14]. Though each of these techniques has proven satisfactory for fabricating devices containing small numbers of valves (< 50), they become impractical in systems where larger numbers of valves (> 100 per chip) are required.

To address this challenge, we have developed a novel ‘slightly-open’ doormat valve (SOD valve) capable of achieving a complete seal, and of regulating the flow of a pressurized gas across a broad range of supply pressures. To demonstrate the utility of this valve design, we have fabricated gas-on-gas multiplexers capable of selectively distending elastomeric membranes by the venting of individual gas-filled channels. To our knowledge, this work represents the first description and demonstration of a SOD valve and gas-on-gas multiplexer.

2. Methods

2.1. SOD valve design and working principle

The control of fluid movement through a SOD valve is afforded by the actuated contact between an elastomeric diaphragm and a patterned discontinuity (the valve seat) within the fluid flow channel. The presence of this discontinuity and diaphragm forces the fluid to either stagnate upstream of this barrier, or to spill over it by causing the

perpendicular displacement of the diaphragm.

The difference between the SOD valve and its NC counterpart lies in the gap height, representing the offset, between the height of the valve seat and the height of the surrounding channel architecture (Fig. 1). The presence of this offset allows the SOD valve to retain the most desired properties of NC valves (i.e. operability at low actuation pressures, compatibility with rectangular channel geometries, insensitivity to channel height), while benefiting from a fabrication technique that allows it to be integrated within microfluidic devices at quantities and densities typically associated with NO valves.

2.2. SU-8 mold fabrication

Fabrication of the multiplexer devices described herein, and of the SOD-valve in general, occurred in two stages: multilayered mold fabrication (Fig. 2A) and device fabrication (Fig. 2B). During the first of these, a silicon wafer (University Wafer, South Boston, MA, USA) was coated with one of several epoxy-based photoresists: SU-8 2 (for molds having target gap heights ranging from 1.5 to 5 microns), SU-8 50 (for molds having target gap heights ranging from 10 to 15 microns) or SU-8 2025 (for molds having target gap heights ranging from 20 to 40 microns) (MicroChem Corp, Newton, MA, USA). These resists were spun at 500 rpm (10 s) and 500–4000 rpm (30 s) to produce features with target heights ranging from 5 to 40 μm using a spin processor (WS-400-6NPP-LITE, Laurell Technologies Corporation, North Wales, PA, USA). Spin protocols used to fabricate molds with specific gap heights were derived from recommended spin velocities provided by the photoresist manufacturer, and the resulting gap heights were confirmed using a stylus profilometer (Dektak XT, Bruker Corporation, Billerica, MA, USA). The SU-8 coated wafer was then placed on a hot plate that was ramped from room temperature (RT) to a surface temperature of 95 °C. The hot plate remained at this temperature for 1–5 minutes, at which point it was shut off to allow its surface (and the wafer) to gradually return to RT (Fig. 2A, left).

A film photomask (CAD/Art Services, Inc, Bandon, OR, USA) was then used in conjunction with a mask aligner system (HTG Hybrid Technologies Corp, San Jose, CA) to selectively expose the coated wafer surface to conventional UV radiation (lamp calibrated 20 mW/cm^2 at 365 nm) for 10–45 seconds. Following UV exposure, the wafer was heated to 95 °C, cooled, and then immersed in SU-8 developer solution (MicroChem Corp, Newton, MA, USA) for 1–10 min s (Fig. 2A, left).

Residual developer solution was then removed using compressed nitrogen gas, and the wafer was again spin-coated with a layer of SU-8 photoresist (i.e. SU-8 2025/2075). This step, and its use of more viscous SU-8 formulations, was intended for the fabrication of features at target

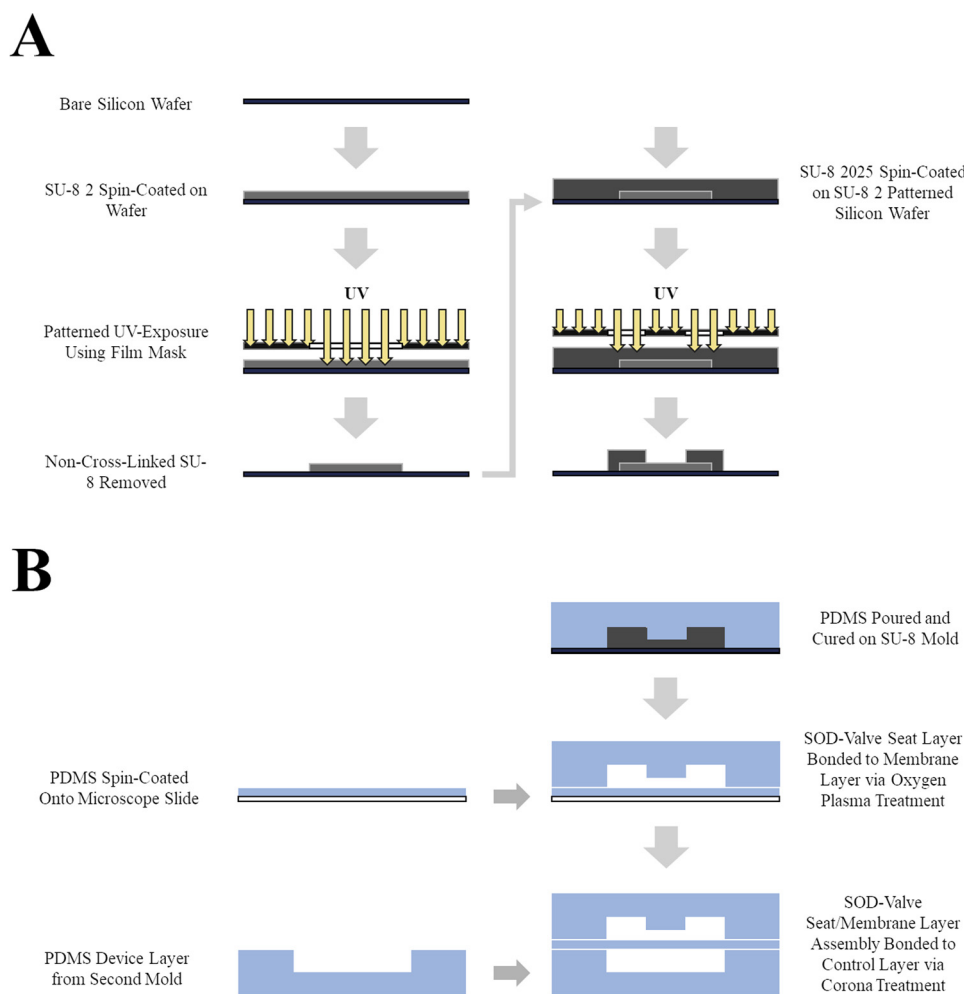


Fig. 2. The fabrication workflow illustrating the fabrication of both the SU-8 mold (A) and multi-layer PDMS device (B).

heights of 50–100 μm . For a target thickness of 100 μm , SU-8 2075 was serially spin-coated at 500 rpm (10 s) and 2100 rpm (30 s) while, for channels having a target thickness of 50 μm , SU-8 2025 was spin-coated at 500 rpm (10 s) and 1750 rpm (30 s). The coated wafer was then placed on a hot plate, ramped to 95 $^{\circ}\text{C}$, and left for 9–20 min s before allowing it to return to RT (Fig. 2A, right).

Once cooled, the non-crosslinked SU-8 was removed from alignment marks positioned near the periphery of the wafer using a circular head swab (ITW Texwipe, Kernersville, NC, USA) dipped in SU-8 developer solution. The alignment marks and workflow utilized herein were developed by Dr. David Lai (unpublished). The wafer was then placed on a hot plate, ramped from RT to 95 $^{\circ}\text{C}$, and left for 5–10 min s. This secondary heating/cooling step ensured that any residual developer solution was removed from the regions surrounding the alignment marks, and consequently minimized the stiction and transference that could otherwise occur between the coated photoresist and the film mask during the UV exposure step. Following UV exposure and development (Fig. 2A, right) performed as was done for the first SU-8 layer, the finished mold was placed in a leveled gravity convection oven (DX-400, Yamato Scientific America, Santa Barbara, CA, USA) for 8–10 hrs at 120 $^{\circ}\text{C}$ and, upon returning to room temperature, was placed in a desiccator for 1 h in the presence of vaporized tridecafluoro-1,1,2,2-tetrahydrooctyl-1-trichlorosilane (United Chemical Tech., Bristol, PA, USA) to ensure passivation of the mold surface.

Fig. 2. Fabrication of Two-Layer Mold and Assembly of PDMS Device.

2.3. PDMS device fabrication

Fabrication of the PDMS device (Fig. 2B) occurred in two stages: fabrication of the patterned channel layers, and fabrication of the elastomeric membrane. During the fabrication of the patterned channel layers, a homogenized 1:10 preparation of PDMS curing agent to prepolymer (Sylgard 184, Dow Corning, Midland, MI, USA) was poured onto the silicon/SU-8 mold to a depth of 2–4 mm. The uncured elastomer/mold was then placed in a leveled gravity convection oven at 60 $^{\circ}\text{C}$ overnight.

During fabrication of the elastomeric membrane, freshly prepared PDMS was spin-coated onto pre-silanized glass slides (silanization of these slides was performed in the same manner as the silanization of the silicon/SU-8 mold described previously) to a target thickness of 20 μm using a CEE-200 spin processor (Brewer Science, Rolla, MO, USA). These coated slides were then cured in a leveled gravity convection oven at 120 $^{\circ}\text{C}$ overnight to ensure complete elastomer curing. This curing process mitigated progressive changes in mechanical properties that could otherwise result from PDMS aging [15,16], and the risk of fabrication defects owed to the use of partially cured elastomeric membranes [15].

The cured PDMS membrane was then bonded via plasma oxygen surface treatment using a vacuum plasma system (Covance MP, FemtoScience, Hwaseong-si, Gyeonggi-do, South Korea) to the patterned layer containing the flow channels. The resulting assembly was then placed in a leveled gravity convection oven at 60 $^{\circ}\text{C}$ for 1–2 hrs, and then carefully removed from the glass slide using a razor blade. By

curing this assembly at 60 °C we were able to avoid the temperature induced shrinkage of patterned PDMS features – relative to their casting mold dimensions – that has been observed when PDMS is cured at higher temperatures [17,18].

This assembly was then bonded to the patterned layer containing the control channels by first treating both bonding surfaces with localized plasma using a Corona SB wand (Elveflow, Paris, France). The importance of using this method for treating the bonding surfaces in lieu of vacuum plasma (as was done when bonding the flow channel layer to the membrane) lay in the ability for corona-treated surfaces to be bonded and de-bonded multiple times in the moments immediately following treatment [19]. This enabled slight misalignments that occurred when manually aligning the control channel layer and flow channel/membrane layer assembly to be corrected prior to formation of a permanent bond. The completed device assembly was then placed in a gravity convection oven at 120 °C overnight to ensure the formation of a permanent bond between all layers.

2.4. Test device designs and assembly of experimental systems

To characterize the functionality and properties of the SOD valve, a series of test devices comprised of single SOD valves positioned at the midpoint of a straight gas-flow channel were fabricated (Fig. 3A). The inlet port was connected to a gas pressure source (P_S) supplying compressed air at 10, 15, or 20 psi via a pressure regulator unit (Model 1500, Teli Dispensing Asia Ltd., Hong Kong), while the outlet port

functioned as a vent – remaining at atmospheric pressure (P_{ATM}). Two perpendicular channels positioned on either side of the valve were connected to piezoelectric pressure sensors (Model ASDXACX030-PAAA5, Honeywell, NJ, USA) to enable monitoring of pressure changes immediately upstream (P_U) and downstream (P_D) of the valve during its operation (Fig. 3A). All connections between the device and external instrumentation (i.e. the liquid dispensing unit and pressure sensors) were made by clear connective tubing (Tygon™ E-3603, Saint-Gobain Performance Plastics, Akron, OH, USA). Analog pressure data was acquired via a multifunction I/O device (USB-6009, National Instruments, Austin, TX, USA), and analyzed using a custom MATLAB script (v2017a, Mathworks, Natick, MA, USA).

All experiments, unless specified otherwise, were performed using compressed nitrogen gas (Item UN1066, Airgas/Air Liquide, Radnor, PA, USA). Additional experiments were performed using compressed carbon dioxide gas (Item UN1013, Airgas/Air Liquide, Radnor, PA, USA), compressed oxygen gas (Item UN1072, Airgas/Air Liquide, Radnor, PA, USA), and compressed atmospheric air (source: filtered intake).

For characterizing the frequency with which the SOD and NC valves could be actuated, the sensitivity of the pressure-based method was found to be insufficient at higher (> 2 Hz) frequencies. This, based upon our initial results, is likely owed to the capacitance of the tubing used to connect the pressure sensors to the test device as the sensitivity seemed to improve when shorter lengths of tubing were used, and to further degrade when longer lengths of tubing were used. Owing to the

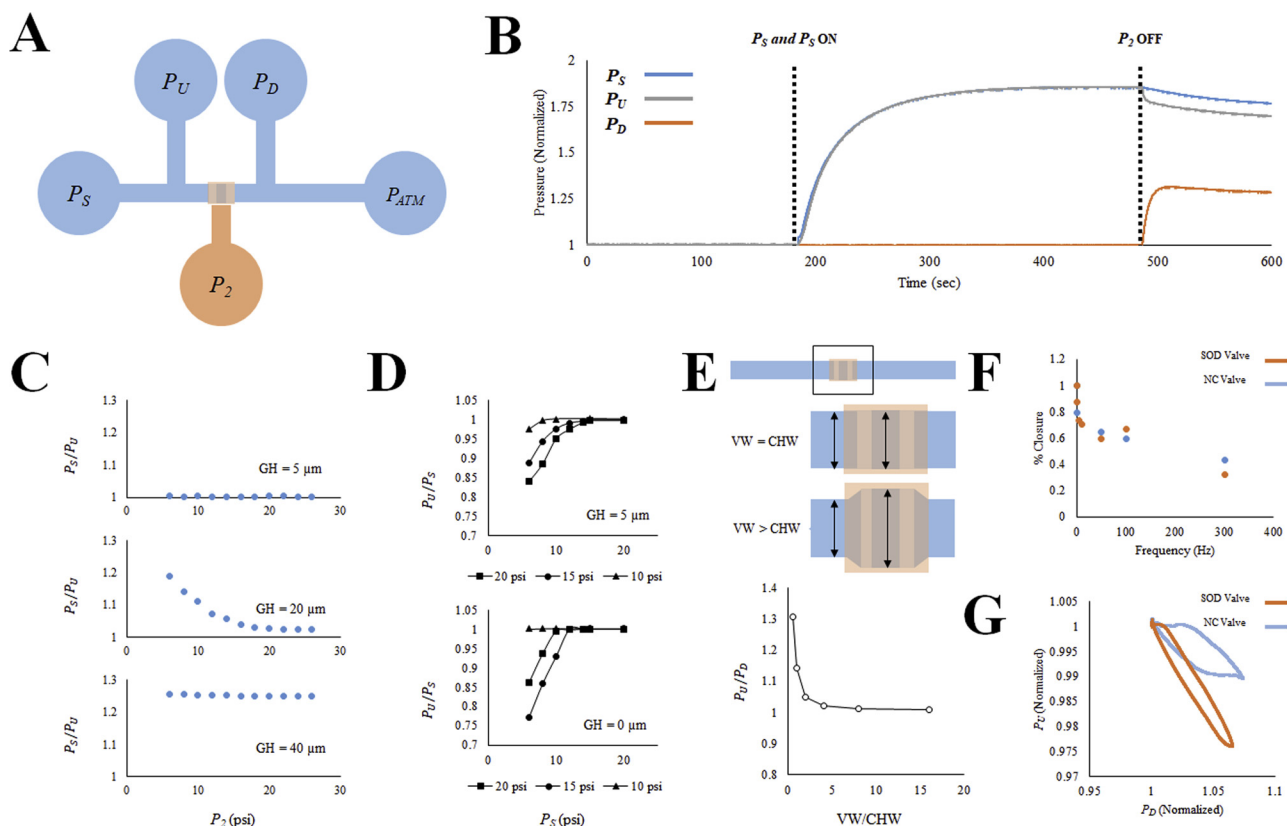


Fig. 3. Utilizing a test device (A), the ability of the SOD valve to achieve and maintain a complete seal was confirmed by applying positive pressure at the inlet while the SOD valve was in a closed state, and monitoring changes in the downstream pressure sensor (P_D). An increase in downstream pressure relative to atmospheric pressure was not observed until the SOD valve was toggled to an open state. (B) SOD valves with gap heights (GH) ranging from 5 to 40 μm were tested to characterize the effect of GH upon the threshold actuation pressure required to achieve closure of the SOD valve. Complete valve closure was observed for GHs $\leq 20 \mu\text{m}$, with the threshold pressure required for actuating the valve being $\leq P_S$. (C) A comparison of the threshold actuation pressure required for closure of the SOD and NC valves indicated no significant difference between these valve designs. (D) The ability to fabricate SOD valves in a manner that doesn't result in an increase in fluidic resistance was verified by fabricating devices with valve widths (VW) greater than the surrounding channel width (CHW). (E) The toggle frequency range across which the SOD valve and NC valve could be operated (F) and hysteresis (both plots are normalized relative to P_S) observed during these changes in valve state (G) were characterized to provide a dynamic comparison of the relative responsiveness of each valve architecture.

superior sensitivity and temporal responsiveness of conductivity measures relative to gas pressure measures [20], test devices containing SOD or NC valves were perfused with a conductive 40 mM KCl solution while 300 μL pipette tips were used to position Ag/AgCl electrodes (Item No. EP05, World Precision Instruments, Sarasota, FL, USA) in the P_U and P_D ports on either side of the valve. A continuous measure of the current between these electrodes allowed the state of the valve to be assessed. The current recorded fluctuated between a high peak value when the valve was held in an open state, and a low baseline value when the valve was held in a closed state. Current recordings were acquired using an electrometer (Model 6514, Keithley Instruments Ltd., Cleveland, OH, USA). To enable the stable actuation of the valve at high frequencies, a function generator (Model AFG320, SONY/Tektronix, Beaverton, OR, USA) was used to provide a 10 V square wave signal to actuate an analog pneumatic valve (Model ITV0010-2BL, SMC, Chiyoda, Tokyo, Japan) connected in-line between an upstream pressure regulator (Model 1500, Teli Dispensing Asia Ltd., Hong Kong) and the test device. All connections were made using clear connective tubing (Tygon™ E-3603, Saint-Gobain Performance Plastics, Akron, OH, USA) and blunt dispensing needle tips (Models JG18-0.5/JG20-0.5, Jensen Global, Santa Barbara, CA, USA).

3. Results and discussion

3.1. The SOD valve can achieve a complete seal

To determine if the SOD valve could achieve a complete seal, the outlet port of a test device (Fig. 3A) was plugged using a PDMS-filled pipette tip. Baseline pressure measurements recorded following the placement of the pipette tip showed $P_S = P_U = P_D = P_{ATM}$. Source pressures ranging from 6 to 20 psi (in 2 psi increments) were then applied while the SOD valve was held in a closed state by 30 psi pressure supplied via the control channel (P_2). Pressure measurements confirmed that $P_U = P_S$ and $P_D = P_{ATM}$ across the range of supply pressures tested. Importantly, these relationships were maintained even when the duration of the applied source pressure exceeded 5 min (Fig. 3B). This indicates that the valve has, indeed, achieved a complete seal and is not simply leaking at a low rate – as such a leak would be expected to produce an increase in P_D relative to P_{ATM} with time. This observation is significant as the ability to generate a complete seal in channels having a rectangular cross section is generally regarded as a fundamental functional advantage of classic NC valves relative to NO valves.

To determine whether the functionality of the SOD valve was dependent upon the gaseous species used to generate the source or control pressures, this experiment was repeated using compressed nitrogen, carbon dioxide, oxygen, and atmospheric air (data not shown). For all experiments, both valve chambers were perfused by a single gaseous species. No species-dependent differences were observed in the functionality of the SOD valve.

3.2. Threshold actuation pressure is dependent on gap height

To determine if, and at what approximate threshold actuation pressure ($P_2 = P_{Th}$), the SOD valve achieved a complete seal, P_S was held at 10, 15, or 20 psi while P_2 was stepped from 6 to 25 psi in 2 psi increments. Following each step increase, the relative pressures at P_S , P_U , P_D , and P_{ATM} were allowed to equilibrate and were then recorded for 30 s. Linear regression was performed to confirm the system had reached a dynamic equilibrium (the predicted slope of a line of best fit being 0 ± 0.001), whereupon the resulting time series data was used to calculate and plot the ratio P_S/P_U as a function of the actuation pressure (P_2) (Fig. 3C). SOD valves with gap heights $\geq 40 \mu\text{m}$ were fabricated, but a complete seal could not be achieved with these devices across the range of actuation pressures tested (Fig. 3C). By modeling the ratios P_U/P_S and P_D/P_{ATM} as functions of P_2 , we then attempted to estimate the true threshold pressure for the SOD and NC valves by calculating the

actuation pressure at which either of these ratios became equivalent to 1 (as would be expected when the valve reached a closed state) (Fig. 3D). For all actuation (P_2) and source (P_S) pressures tested, $P_{Th} \leq P_S$ when the SOD valve gap height is below $20 \mu\text{m}$ – with no significant difference in P_{Th} when comparing NC and SOD valves with gap heights as large as $5 \mu\text{m}$ (Fig. 3D).

3.3. SOD valves may be designed to eliminate valve-associated baseline channel resistance

Conventional NC valves typically increase channel resistance due to the resting contact between the elastomeric membrane and the valve ‘seat’. This contact force must be overcome for flow to proceed through the valve. SOD valves, by eliminating this resting contact and supporting a range of widths and gap-heights, may be designed such that the resistance of the valve does not exceed the baseline hydraulic resistance of the channel. To demonstrate this phenomenon, the ratio between the upstream and downstream pressures was recorded for test devices containing valves with $5 \mu\text{m}$ gap heights and channel widths ranging from $200 \mu\text{m}$ to 3.2 mm. By calculating the pressure drop across these valves (in their resting state), we demonstrate that for a fixed gap height, increasing the width of the valve can effectively increase the hydraulic radius of the channel such that the pressure drop across the valve approaches zero (Fig. 3E).

3.4. SOD valves may be actuated at frequencies comparable to NC valves

The ability to reliably toggle the state of NC valves between fully open and closed states at low pressures, and frequencies ≥ 1 Hz, presents a distinct functional advantage relative to NO valves where actuation at high frequencies requires the use of either shallow flow channels or high actuation pressures. To compare the frequency range across which SOD and NC valves may be operated, test devices containing SOD valves (GH = $5 \mu\text{m}$) or NC valves were toggled between open and closed states at frequencies ranging from 0.5 to 300 Hz. Complete closure was observed at frequencies ranging from 0.5 to 2 Hz, while partial closure without loss of synchrony between the valve state and applied pressure waveform was achieved at frequencies as high as 300 Hz. Importantly, there was no ostensible difference in the frequency range across which the SOD valve could be toggled relative to the NC valve, and no ostensible difference in the frequency range across which full or partial valve closure was observed. (Fig. 3F).

Hysteresis was observed in the operation of both SOD and NC valves when using a pressure-based method for assessing valve closure. Though the magnitude of hysteresis observed in both valves was minimal, greater hysteresis was observed in the operation of NC valves relative to SOD valves (Fig. 3G). This hysteresis may be owed to the stiction that occurs between the membrane and valve seat when the valve is in its resting state as the maximum frequency at which the NC valve could be toggled in a liquid-driven/wet state (where the liquid present may act to lubricate the contact between the membrane and valve seat) does not ostensibly differ from that of the NC valve. The maximum actuation frequency of both valves at frequencies exceeding 1–2 Hz could not be accurately measured in a gas-driven/dry state test device.

3.5. SOD valves enable the simple fabrication of gas-on-Gas multiplexers

To demonstrate the fabrication efficiency and functional utility of the SOD valve, we designed an elastomeric balloon array wherein a source pressure sufficient to constitutively distend (inflate) all balloon elements within the array could be selectively vented to allow for the relaxation (deflation) of individual balloon elements using a gas-on-gas multiplexer (Fig. 4A). The functional unit of this system is a straight channel that originates at a common inlet and terminates at a unique outlet held at atmospheric pressure. Immediately upstream of each

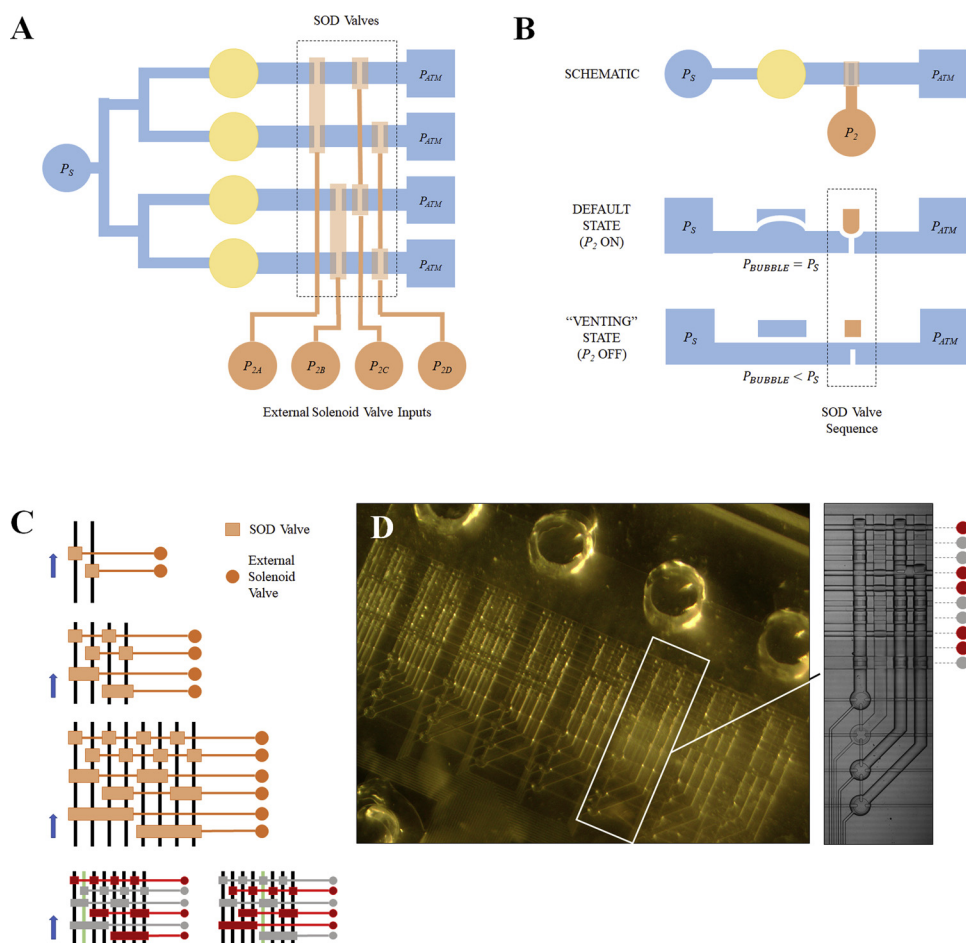


Fig. 4. (A) A simplified schematic of the gas-on-gas multiplexer where pressure supplied via a common inlet port (P_S) is distributed to four unique flow channels that terminates at a unique outlet port (P_{ATM}). Each flow channel contains one balloon element (yellow circle) upstream of the SOD valve region. The state of each SOD valve can be toggled by a series of external solenoid valves (P_{2A-D}). (B) The functional element of the gas-on-gas multiplexer is a flow channel connecting a common pressure source (P_S) to a unique outlet port (P_{ATM}). The overhead schematic of this functional unit (top) illustrates the relative positions of the inlet (P_S), balloon element (yellow circle), SOD valve region, external solenoid input (P_2), and outlet (P_{ATM}). The side-view schematics illustrate how closure of the SOD valve via the external solenoid valve (P_2) can raise the pressure in the upstream region of the flow channel to the source pressure (middle), while opening of the SOD valve can allow for relaxation of the balloon element by allowing the pressure in the channel to vent via the outlet port (P_{ATM}) (bottom). (C) The scalable multiplexer control scheme allows for the selective venting of n flow channels (black) using $2\log_2 n$ external solenoid valves (orange circles). The schematics shown illustrate the scalability of this system (where 2 flow channels can be regulated using 2 external valves, 4 flow channels can be regulated using 4 external valves, and 8 flow channels can be regulated using 6 external valves) and how the closure of a specific sequence of solenoid valves can allow an operator to selectively vent single flow channels. Red solenoid inputs and SOD valves are in an ON (positive pressure) state while gray inputs and SOD valves are in an OFF (atmospheric pressure) state. The green flow channels represent the venting channels as defined by the sequence of external solenoid valves shown. Blue arrows represent the direction of the pressure gradient – arrows point from the pressure source (P_2) to the channel outlets (P_{ATM}). (D) Photographs illustrating the design and operation of the elastomeric balloon array and gas-on-gas multiplexer device containing 160 SOD valves capable of toggling the state of 32 flow channels using 10 external solenoid valves. In the upper device layer, red regions represent channels connected to external solenoid valves that are in an ON (positive pressure) state, while gray regions represent channels connected to external solenoid valves that are in an OFF (atmospheric pressure) state (For interpretation of the references to colour in this figure legend, the reader is referred to the web version of this article).

outlet is a sequence of SOD valves that can be actuated via external solenoid valves. When one or more of these SOD valves are in a closed state, the pressure within the upstream channel region approaches the source pressure supplied at the inlet port. When these SOD valves are in an open state, the upstream channel becomes continuous with the outlet, allowing the channel pressure to approach the outlet pressure. By positioning a single balloon element between the inlet and the SOD valve region of each functional unit, we enabled the pressure within each element to be toggled by changing the state of the downstream SOD valves (Fig. 4B). Each functional unit was designed to accommodate 5 SOD valves, arranged according to a binary control scheme capable of toggling the state of n balloon elements using $2\log_2 n$ external solenoid valves (Fig. 4C) [21].

The ability to toggle the state of each balloon element requires that the pressure drop between the balloon element and outlet/vent is

greater than the pressure drop between the balloon element and the common pressure source. That, in other words, the pressure driven gas flow supplied to each balloon element from the source is vented faster than it is supplied – thereby ensuring that the pressure at a balloon element never reaches the threshold pressure required to distend the valve membrane when its corresponding flow channel is actively venting. To achieve this, the device reported herein was designed such that the ratio between the calculated hydrodynamic resistance upstream and downstream of each balloon element was approximately 15.

To assess the fabrication efficiency of multiplexers containing SOD valves, over 20 devices (each device containing 160 SOD valves) were fabricated (Fig. 4D). Of these, all devices (containing over 3200 valves in total) were found to be fully functional.

4. Conclusions

The work reported herein represents, to our knowledge, the first description of a SOD valve, and of a functional (and highly scalable) gas-on-gas multiplexer. The scalability of this design is owed to the use of a novel strategy for mitigating the risk of bonding between the valve 'seat' and elastomeric membrane that currently limits the fabrication efficiency and scalability of monolithic NC valves, and to the minimal design constraint presented by the need to balance the ratios between the upstream and downstream channel resistance of the valves being operated using the gas-on-gas multiplexer. Within the scope of the work reported herein, this approach has allowed us to design and operate a device containing 32 node valves controlled by a multiplexer containing 160 SOD valves using only 10 external solenoid valves and a single common pressure source.

Our observation that the functionality of the SOD valve is solely dependent upon the pressure differential between the flow/regulated (P_3) and control/regulating (P_2) valve chambers – and not upon the chemical species present within either chamber – suggests these valves could be utilized to enable high throughput applications where the controlled delivery of specific gaseous species may be desired. For such applications, however, the permeability of PDMS to multiple gaseous species [22,23] may necessitate the use of appropriate mitigation strategies to prevent mixing across PDMS barriers (e.g. the elastomeric membrane) where, for example, one gaseous species is used to regulate another. In addition, as the complexity of microfluidic systems increases – particularly in areas of high-throughput analyses and soft robotics, the need for efficient valving (both in terms of fabrication and operability) could be addressed by the SOD valve.

Author contributions

P.W. developed, designed, and fabricated devices. P.W. and T.K. performed experiments and data analysis. P.W. wrote the manuscript, and all authors contributed equally to editing the manuscript.

Acknowledgements

The authors extend their gratitude to Dr. David Lai (GSK), who developed the multi-layer mold fabrication technique described herein, and to Mr. Arpith Vedhanayagam, who assisted with conducting and troubleshooting multiple experiments. The authors are also grateful to Mr. Stephen Robinson, Dr. Sung-Jin Kim and Dr. Sasha Cai Leshner-Perez for thoughtful conversations and shared insight throughout the conceptual development and practical execution of the work reported herein.

This work was supported by the National Science Foundation Division of Chemical, Bioengineering, Environmental, and Transport Systems (CBET) under award numbers 1236764 and 1512544.

Appendix A. Supplementary data

Supplementary material related to this article can be found, in the online version, at doi:<https://doi.org/10.1016/j.snb.2019.126776>.

References

- [1] C.-W. Tsao, Polymer microfluidics: simple, low-cost fabrication process bridging academic lab research to commercialized production, *Micromachines* 7 (225) (2016) 1–11.
- [2] M.A. Unger, H.-P. Chou, T. Thorsen, A. Scherer, S.R. Quake, Monolithic micro-fabricated valves and pumps by multilayer Soft lithography, *Science* 288 (5463) (2000) 113–116.
- [3] I.E. Araci, S.R. Quake, Microfluidic very large scale integration (mVLSI) with integrated micromechanical valves, *Lab Chip* 12 (2012) 2803–2806.
- [4] K. Hosokawa, R. Maeda, A normally closed PDMS (Polydimethylsiloxane) micro-valve, *IEEE Trans. Sens. Micromachines* 120 (4) (2000) 177–178.
- [5] B.-H. Jo, L.M. Van Lerberghe, K.M. Motsegood, D.J. Beebe, Three-dimensional micro-channel fabrication in polydimethylsiloxane (PDMS) elastomer, *J. Microelectromechanical Syst.* 9 (1) (2000) 76–81.
- [6] D.C. Duffy, J.C. McDonald, O.J. Schueller, G.M. Whitesides, Rapid Prototyping of Microfluidic Systems in Poly(dimethylsiloxane), *Anal. Chem.* 70 (23) (1998) 4974–4984.
- [7] H. Ye, Z. Gu, D.H. Gracias, Kinetics of Ultraviolet and Plasma Surface Modification of Poly(dimethylsiloxane) Probed by Sum Frequency Vibrational Spectroscopy, *Langmuir* 22 (4) (2006) 1863–1868.
- [8] B. Mosadegh, H. Tavana, S.C. Leshner-Perez, S. Takayama, High-density fabrication of normally closed microfluidic valves by patterned deactivation of oxidized polydimethylsiloxane, *Lab Chip* 11 (2011) 738–742.
- [9] A. Jahanshahi, P. Salvo, J. Vanfleteren, PDMS selective bonding for the fabrication of biocompatible all polymer NC microvalves, *J. Microelectromechanical Syst.* 22 (6) (2013) 1354–1360.
- [10] Y.-N. Yang, S.-K. Hsiung, G.-B. Lee, A pneumatic micropump incorporated with a normally closed valve capable of generating a high pumping rate and a high back pressure, *Microfluid. Nanofluidics* 6 (6) (2009) 823–833.
- [11] D. Irimia, M. Toner, Cell handling using microstructured membranes, *Lab Chip* 6 (2006) 345–352.
- [12] R. Samuel, C.M. Thacker, A.V. Maricq, B.K. Gale, Simple and cost-effective fabrication of microvalve arrays in PDMS using laser cut molds with application to C. Elegans manipulation in microfluidics, *J. Micromechanics Microengineering* 24 (2014) 1–11.
- [13] C.I. Rogers, J.B. Oxborrow, R.R. Anderson, L.-F. Tsai, G.P. Nordin, A.T. Woolley, Microfluidic valves made from polymerized polyethylene glycol diacrylate, *Sens. Actuators B Chem.* 191 (2014) 1–19.
- [14] R. Mohan, B.R. Schudel, A.V. Desai, J.D. Yearsley, C.A. Appleby, P.J.A. Kenis, Design considerations for elastomeric normally closed microfluidic valves, *Sens. Actuators B Chem.* 160 (no. 1) (2011) 1216–1223.
- [15] I.D. Johnston, D.K. McCluskey, C.K.L. Tan, M.C. Tracey, Mechanical characterization of bulk sylgard 184 for microfluidics and microengineering, *J. Micromechanics Microengineering* 24 (3) (2014) 035017 1–7.
- [16] D.T. Eddington, W.C. Crone, D.J. Beebe, Development of process protocols to fine Tune polydimethylsiloxane material properties, 7th International Conference on Miniaturized Chemical and Biochemical Analysis Systems, Squaw Valley, California, USA, (2008).
- [17] C. Moraes, Y. Sun, C.A. Simmons, Solving the shrinkage-induced PDMS alignment registration issue in multilayer Soft lithography, *J. Micromechanics Microengineering* (2009) 065015.
- [18] S.W. Lee, S.S. Lee, Shrinkage ratio of PDMS and its alignment method for the wafer level process, *Microsyst. Technol.* 14 (2) (2008) 205–208.
- [19] C. Yang, W. Wang, Z. Li, Optimization of corona-triggered PDMS-PDMS bonding method, *IEEE International Conference on Nano/Micro Engineered and Molecular Systems*, Shenzhen, China, (2009).
- [20] L.A. Godwin, K.S. Deal, L.D. Hoepfner, L.A. Jackson, C.J. Easley, Measurement of microchannel fluidic resistance with a standard voltage meter, *Anal. Chim. Acta* 758 (2013) 101–107.
- [21] T. Thorsen, S.J. Maerkl, S.R. Quake, Microfluidic large-scale integration, *Science* 298 (5593) (2002) 580–584.
- [22] T.C. Merkel, V.I. Bondar, B.D. Freeman, I. Pinnau, Gas Sorption, Diffusion, and Permeation in Poly(Dimethylsiloxane), *J. Polym. Sci. Part B: Polym. Phys.* 38 (3) (2000) 415–434.
- [23] K.S. Houston, D.H. Weinkauf, F.F. Stewart, Gas Transport Characteristics of Plasma Treated Poly(Dimethylsiloxane) and Polyphosphazene Membrane Materials, *J. Memb. Sci.* 205 (1–2) (2002) 103–112.